A Novel Hybrid Unsupervised Domain Adaptation Method for Cross-subject Joint Angle Estimation from Surface Electromyography

Long Wang, Xiaoling Li, Zhangyi Chen, Zhipeng Sun, Jingyi Xue, Wei Sun, Shiwen Zhang, Jiajia Sun, and Guimin Chen, *Member, IEEE*

***Abstract*—Individual physiological differences constrain the cross-user application of joint angle estimation models based on surface electromyography (sEMG) signals. Current cross-user methods for myoelectric joint angle estimation often involve the use of angle or optical sensors, which increases the training burden and costs for new users. To enable new users to perform joint angle estimation solely using sEMG sensors, this study proposes a hybrid unsupervised domain adaptation network that combines multi-order metric and adversarial mechanisms (MADAN). MADAN aims to minimize the distribution differences of sEMG signals between the source and target subjects by first aligning the domain distributions and then increasing domain confusion. The effectiveness of MADAN is validated through cross-subject wrist joint angle estimation involving 10 subjects, with an estimation frequency of 20Hz. The results demonstrate that MADAN achieves a significantly higher average coefficient of determination (0.8688 ± 0.0307) compared to other advanced UDA cross-subject estimation methods, such as TCDA (0.6534 ± 0.234) and ADANN (0.6655 ± 0.2255). Notably, MADAN requires only 20 seconds of unlabeled samples from the target subject for training. This work is expected to alleviate the cost and training burden for new users in performing myoelectric continuous motion estimation.**

***Index Terms*—sEMG, joint angle estimation, cross-subject, unsupervised domain adaptation (UDA)**

I. Introduction

Surface electromyography (sEMG) signals can decode human motion intention and have found extensive application in prosthetics and robot control [1]. Motion intention estimation based on sEMG includes discrete and continuous motions. Compared with discrete motion, continuous motion estimation can be used for synchronous or proportional control of robots and dexterous hands [2, 3].

In recent years, deep learning (DL) has been extensively used for myoelectric continuous motion estimation [4-6]. However, most studies have focused on improving recognition accuracy [7, 8], while paying less attention to the practical applicability of these approaches. It is important to note that sEMG-based human-machine interaction systems often encounter various non-ideal factors in real-world settings, including individual differences [9, 10], electrode displacement [11, 12], muscle fatigue [13], and limb posture [14, 15]. These factors can significantly compromise the performance of motion estimation. Among these non-ideal factors, individual differences are inevitable. Individual physiological parameters such as muscle density, fat content, and arm length can influence the distribution of sEMG signals among subjects [16, 17]. This poses a challenge for the cross-user application of DL methods, as they typically assume that the training and test datasets have similar distributions. As a result, when applying a trained DL model to estimate new users, the performance may significantly decrease due to variations in the distribution of sEMG signals among subjects. The current solution for scenarios involving new users typically involves collecting new training data to calibrate the model [18]. However, this requirement imposes a heavy training burden on users, leading many individuals to abandon the use of myoelectric products [19].

The recent development of transfer learning (TL) has provided an effective solution for improving the generalization capability of DL methods to new tasks. Domain adaptation, one of the research directions in TL, defines a domain with abundant labels as the source domain and a domain with limited or no labels as the target domain [20]. Domain adaptation aims to extract common latent features from source and target domains to enable cross-domain estimation [21]. Some researchers have developed domain adaptation-based myoelectric motion estimation methods to handle cross-subject scenarios [22, 23]. Long et al. [24] proposed a method based on adversarial knowledge transfer learning for cross-subject estimation of finger joint angles. Bao et al. [25] proposed a two-stream convolutional neural network (CNN) model with an embedded domain discrepancy loss, which enables cross-subject wrist angle estimation by extracting domain-invariant features. However, these methods are based

Manuscript received April 4, 2023; Revised July 7, 2023; Accepted September 5, 2023. This paper was recommended for publication by Editor Angelika Peer upon evaluation of the Associate Editor and Reviewers' comments. This work was funded by Key R&D project of Shaanxi Province (2023-YBGY-505). *(Corresponding author: Xiaoling Li.)*

Long Wang, Xiaoling Li, Zhangyi Chen, Zhipeng Sun, Jingyi Xue, Wei Sun, Shiwen Zhang and Guimin Chen are with the School of Mechanical Engineering, Xi'an Jiaotong University, Xi'an 710049, China. (e-mail: wangl521@stu.xjtu.edu.cn;xjtulxl@mail.xjtu.edu.cn;3120101240@stu.xjtu.edu.cn;szp9904@stu.xjtu.edu.cn;1004468304@qq.com;a160680243@163.com; 1748337396@qq.com; guimin.chen@xjtu.edu.cn).

Jiajia Sun is with the State Key Laboratory of Electrical Insulation and Power Equipment, Xi'an Jiaotong University, Xi'an 710049, China. (e-mail: sunjiajia@xjtu.edu.cn).

Digital Object Identifier (DOI): see top of this page.

on supervised domain adaptation (SDA), which requires collecting both sEMG and joint angle data from new subjects to implement the proposed methods. Although the authors in [25] mention the possibility of improving their method into an unsupervised domain adaptation (UDA) approach, they do not provide any results or performance comparisons.

In cross-subject continuous motion estimation, the ideal objective is to achieve excellent estimation performance using only a small amount of sEMG data collected from new users. This would eliminate the need for new users to wear additional sensors to obtain label information, thereby reducing the cost and burden associated with using myoelectric products. To achieve this objective, we consider the UDA method to be a promising solution [26]. It everages the knowledge learned from the source subjects and transfers it to the target subjects, facilitating knowledge transfer without requiring label information from the target subjects.

In UDA-based cross-subject joint angle estimation, attention should be given to two problems: (1) establishing an accurate mapping relationship between sEMG data and joint angles, and (2) minimizing the differences in sEMG signal distributions between subjects to reduce the impact of individual differences on model performance. To address these problems, the following requirements were identified for the proposed method. Firstly, it was observed that the previous moment's sEMG signal significantly influences the current joint angle estimate. Therefore, the proposed method must be capable of extracting time-dependent features from the sEMG signal. Secondly, it has been demonstrated that the sEMG signal exhibits significant inter-subject variability, with varying degrees of difference between different subjects [22]. Consequently, the proposed method must be effective in reducing the varying degrees of differences among the subjects.

To achieve the above requirements, this work proposes a UDA method named domain adaptive network with multi-order metric and adversarial mechanism (MADAN). MADAN extracts sEMG features using a Bidirectional Gate Recurrent Unit (BiGRU). Furthermore, it incorporates a multi-order metric and an adversarial mechanism to align domain distributions and increase domain confusion, respectively. The objective of the proposed method is to achieve unsupervised estimation of joint angles for target subjects by minimizing inter-subject differences.

II. METHODS

A. Problem Definition

We consider the following problem of cross-subject myoelectric joint angle estimation. Given a labeled source domain $\mathcal{D}_S = \{x_S^i, y_S^i\}_{i=1}^{N_S}$ that obeys the distribution $P_S(x,y)$ and has a sample size N_S. Given an unlabeled target domain $\mathcal{D}_T = \{x_T^i\}_{i=1}^{N_T}$ that obeys the distribution $P_T(x,y)$ and has a sample size N_T. The source domain contains sEMG data and joint angles, whereas the target domain contains only sEMG data. Individual differences lead to a different joint distribution of source and target domains ($P_S(x,y) \neq P_T(x,y)$).

This work aims to employ $\mathcal{D}_S = \{x_S^i, y_S^i\}_{i=1}^{N_S}$ and $\mathcal{D}_T = \{x_T^i\}_{i=1}^{N_T}$ learn an estimation function f, which has the minimum estimation error in the test dataset $\mathcal{D}_{test} = \{x_{test}^i, y_{test}^i\}_{i=1}^{N_{test}}$ that obeys the distribution $P_T(x,y)$, namely

$$f^* = \arg\min_{f \in \mathcal{H}} \mathbb{E}_{(x_i, y_i) \in \mathcal{D}_{test}} L_y(f(x_i), y_i) \tag{1}$$

where $\mathcal{H}$ is the hypothesis space, L_y is the loss function of joint angle estimation.

B. Proposed Model

The proposed MADAN consists of three main modules: a feature extraction module, a domain-invariance learning module, and a joint angle estimation module. A detailed description of each module is provided below.

1) Feature extraction module

Long Short-Term Memory (LSTM) and Gate Recurrent Unit (GRU) are special variants of Recurrent Neural Network (RNN). LSTM solves the problem of RNN gradient disappearance and explosion by introducing three gate units (input gate, forgetting gate and output gate). GRU achieves the same function by introducing only two gate units (update gate and reset gate). LSTM and GRU demonstrate comparable feature extraction performance at optimal hyperparameters. However, GRU has fewer weighting parameters than LSTM and is easier to implement. In addition, previous studies have shown that bidirectional recurrent neural networks are more suitable for extracting sEMG features [4, 5]. Therefore, MADAN introduces BiGRU to extract myoelectric features from both the source and target subjects.

2) Domain-invariance learning module

a) Metric-based domain alignment: Maximum Mean Discrepancy (MMD) is defined as the mean embedding distance of two distributions p and q mapped onto the reproducing kernel Hilbert space (RKHS) [27]. Given a source domain $\mathcal{D}_S = \{x_S^i\}_{i=1}^{N_S}$ and a target domain $\mathcal{D}_T = \{x_T^i\}_{i=1}^{N_T}$, the squared form of the MMD is defined as

$$l_{MMD} = \left\| \frac{1}{N_S} \sum_{x_S^i \in \mathcal{D}_S} \phi(x_i) - \frac{1}{N_T} \sum_{x_T^i \in \mathcal{D}_T} \phi(x_i) \right\|_{\mathcal{H}_k}^2 \tag{2}$$

where $\mathcal{H}_k$ represents the RKHS with the characteristic kernel k. A Gaussian kernel was adopted for this work. The mapping function $\phi(\cdot)$ defines a mapping from the original data to the RKHS.

Correlation alignment (CORAL) is defined as the distance between the second-order covariance of the source and target domains [28].

$$l_{CORAL} = \frac{1}{4m^2} \left\| C_S - C_T \right\|_F^2 \tag{3}$$

where $\|\cdot\|_F^2$ and m represent the squared matrix Frobenius norm and dimension of the input features, respectively. C_S and C_T represent the covariance matrices of the source and target domains, respectively.

$$C_s = \frac{1}{N_s - 1}\left(\mathcal{D}_S^{\mathrm{T}} \mathcal{D}_S - \frac{1}{N_s} (\mathbf{1}^{\mathrm{T}} \mathcal{D}_S)^{\mathrm{T}} (\mathbf{1}^{\mathrm{T}} \mathcal{D}_S) \right) \tag{4}$$

$$C_T = \frac{1}{N_T - 1}\left(\mathcal{D}_T^{\mathrm{T}} \mathcal{D}_T - \frac{1}{N_T} (\mathbf{1}^{\mathrm{T}} \mathcal{D}_T)^{\mathrm{T}} (\mathbf{1}^{\mathrm{T}} \mathcal{D}_T) \right) \tag{5}$$

where $\mathbf{1}$ represents the unit vector.

MMD is the first-order statistical difference between the source and target domain distributions, whereas CORAL is the second-order statistical difference. Here, we propose a metric domain adaptation based on multi-order statistical moments, which combines first-order MMD and second-order CORAL loss. The multi-order metric is defined as

$$L_{multi-order} = l_{MMD} + \gamma \cdot l_{CORAL} \tag{6}$$

where γ is the multi-order trade-off parameter.

b) Adversarial-based domain confusion: The H-divergence measures domain distribution discrepancy from the perspective of domain confusion [29]. Because H-divergence is challenging to calculate, distance minimization based on domain confusion is typically achieved through domain adversarial training [30, 31]. Domain adversarial neural network generally consists of a feature extractor and a domain discriminator [31]. The feature extractor is applied to extract source and target domain features. The domain discriminator is a binary classification network to determine whether the input features are from the source or target domain. The loss function is the binary cross-entropy.

$$L_d = \frac{1}{n}\sum_{i=1}^{n} \left(d_i \log \frac{1}{\hat{d}_i} + (1 - d_i) \log \frac{1}{1 - \hat{d}_i} \right) \tag{7}$$

where d_i and $\hat{d}_i$ denote actual and predictive domain labels, respectively.

A gradient reversal layer (GRL) is introduced between the domain discriminator and the feature extractor to update the weight parameters. In the forward propagation process, GRL is equivalent to an identity change, defined as

$$R_\lambda(x) = x \tag{8}$$

In the backpropagation process, GRL becomes negative after solving the gradient, defined as

$$\frac{dR_\lambda}{dx} = -\lambda I \tag{9}$$

where λ is the domain adversarial trade-off parameter.

As a result, the domain discriminator minimizes the domain classification loss, and the feature extractor maximizes it through the GRL. Domain confusion is realized when the domain discriminator cannot correctly discriminate which domain the input features come from.

c) Hybrid domain adaptation: The metric-based domain alignment reduces the inter-domain distance directly, thus achieving a better alignment of two distributions with large discrepancies. However, it cannot achieve better domain confusion as the adversarial mechanism. In contrast, the adversarial mechanism effectively confuses the two domain features, making it suitable for handling tasks with minor shifts, but it may not be able to reduce larger inter-domain shifts [32].

Given that the distribution shift of sEMG signals due to individual differences can vary in magnitude, it is necessary to develop a UDA method capable of handling various levels of domain shift. This work proposes a hybrid UDA method combining the multi-order metric and adversarial mechanism, leveraging their strengths to reduce domain shifts.

3) Joint angle estimation module

The joint angle estimation module is a fully connected regression network that establishes a mapping between the domain-invariant features and the joint angle. The joint angle estimation loss is the mean square error.

$$L_y = \frac{1}{n}\sum_{i=1}^{n} (y_i - \hat{y}_i)^2 \tag{10}$$

where n is the batch size of the training set. y_i and $\hat{y}_i$ denote the ground-truth and the estimated joint angle, respectively.

4) Training of MADAN

MADAN contains three optimization objectives: (1) joint angle estimator loss L_y; (2) multi-order metric domain adaptation loss $L_{multi-order}$; (3) domain discriminator loss L_d. The training procedure is presented in Algorithm 1.

Algorithm 1: Training Procedure of MADAN

Input: A labeled source domain $\mathcal{D}_S = \{x_S^i, y_S^i\}_{i=1}^{N_S}$, an unlabeled target domain $\mathcal{D}_T = \{x_T^i\}_{i=1}^{N_T}$, batch size n_b.

1: Initialize $\{\theta_f, \theta_d, \theta_y\}$ of MADAN
2: **for** epoch=1,2,…,max_epoch do:
3: Sample $\{x_S^i, y_S^i\}_{i=1}^{n_b}$, a batch from the source dataset $\mathcal{D}_S$.
4: Sample $\{x_T^i\}_{i=1}^{n_b}$, a batch from the target dataset $\mathcal{D}_T$.
5: Update θ_f using $\{x_S^i\}_{i=1}^{n_b}$ and $\{x_T^i\}_{i=1}^{n_b}$ by (13).
6: Update θ_f and θ_y using $\{x_S^i, y_S^i\}_{i=1}^{n_b}$ by (14).
7: Update θ_d using $\{x_S^i\}_{i=1}^{n_b}$ labeled with ' 0 ' and $\{x_T^i\}_{i=1}^{n_b}$ with ' 1 ' by (15).
8: **end**

Output: Optimal weights $\{\theta_f, \theta_d, \theta_y\}$

In one epoch, the parameters are optimized in two steps. The first-step loss function is

$$L_{loss1}(\theta_f) = L_{multi-order} \tag{11}$$

The second-step loss function is

$$\begin{aligned} L_{loss2}(\theta_f, \theta_y, \theta_d) = & \sum_{x_i \in \mathcal{D}_S} L_y(G_y(G_f(x_i)), y_i) \\ & - \lambda \sum_{x_i \in \mathcal{D}_S \cup \mathcal{D}_T} L_d(G_d(G_f(x_i)), d_i) \end{aligned} \tag{12}$$

where θ_f , θ_y , θ_d are the weight parameters of the feature extraction network G_f , the joint angle estimation network G_y and the discriminator network G_d , respectively.

First, L_{loss1} is minimized to align the distribution of the source and target domains.

$$(\hat{\theta}_f) = \arg\min_{\theta_f} L_{loss1}(\theta_f) \tag{13}$$

Second, L_d is maximized to confuse the source and target domains further, while L_y is minimized to learn the mapping relationship between sEMG features and joint angles. This max-min optimization process is implemented via GRL.

$$(\hat{\theta}_f, \hat{\theta}_y) = \arg\min_{\theta_f, \theta_y} L_{loss2}(\theta_f, \theta_y, \hat{\theta}_d) \tag{14}$$

$$(\hat{\theta}_d) = \arg\max_{\theta_d} L_{loss2}(\hat{\theta}_f, \hat{\theta}_y, \theta_d) \tag{15}$$

In summary, Fig. 1 provides a visual representation of the structure and training process of the proposed method.

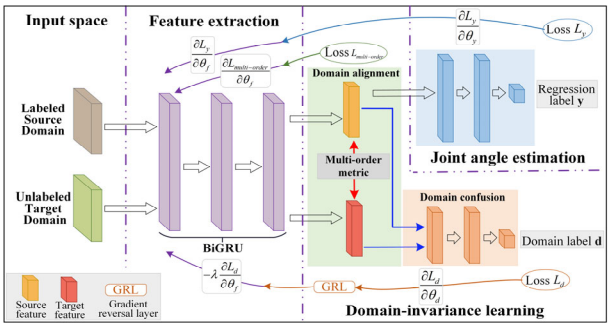

Fig. 1. The structure and workflow of the proposed MADAN.

C. Flowchart of Joint Angle Estimation

Fig. 2 presents the flowchart for cross-subject myoelectric joint angle estimation using the proposed MADAN method. In practical applications, it is assumed that labeled data from source subjects are available, while the target subject only needs to wear sEMG sensors and perform three complete wrist flexion and extension exercises to collect calibration data. The estimation model is then trained using the unlabeled data from the target subject and the labeled data from the source subjects. Subsequently, the trained model is used by the target subject to estimate the wrist joint angle, which can be utilized for controlling a robot to achieve synchronous or proportional motion.

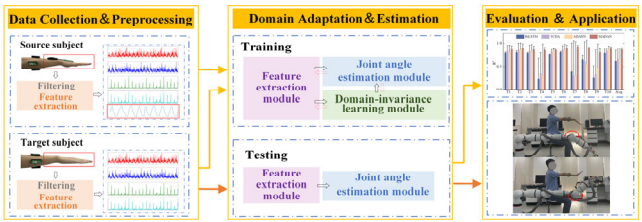

Fig. 2. Flowchart of MADAN applied to cross-subject joint angle estimation.

III. Experiments

A. Experimental Setup

Ten healthy subjects participated in the experiment. The main information of the 10 selected subjects includes gender (6 males and 4 females), age (22-26 years), weight (45-81 kg), height (158-187 cm), arm length from the elbow joint to the wrist joint (23.2-27.8 cm), and arm circumference at the midpoint of the wrist and elbow joints (20.4-26.5 cm). All subjects were informed in detail of the purpose and process of the experiment and signed a consent form which Xi'an Jiaotong University Ethics Committee Data Acquisition approved.

A DataLITE system from Biometrics simultaneously recorded the sEMG data and wrist angles. Four DataLITE wireless sEMG sensors with a sampling frequency of 2000 Hz were used to collect sEMG signals. As shown in Fig. 3, with reference to the motor anatomy, four sEMG sensors were placed on the four major muscles that control wrist movement. A DataLITE wireless angle sensor with a sampling frequency of 1000 Hz was used to capture the wrist angle.

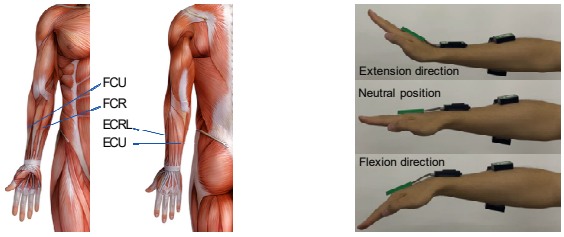

Fig. 3. The signal acquisition scheme. (a) The principal muscles that control wrist movement are extensor carpi ulnaris (ECU), extensor carpi radialis longus (ECRL), flexor carpi radialis (FCR), and flexor carpi ulnaris (FCU). (b) A complete wrist flexion and extension motion.

A complete wrist flexion and extension motion was defined as follows: rotating the wrist from a neutral position in the flexion direction, then rotating it in the extension direction, and finally returning to the neutral position. During signal acquisition, subjects performed flexion and extension movements of the right wrist, which took approximately 6 seconds for each complete movement. Each experiment lasted 65 seconds with a 30 seconds rest, and two trials were recorded for each subject. Therefore, a total of 130 seconds of data were collected from each subject.

B. Preprocessing and Feature Extraction

According to common settings reported in the literature [25, 33], we used a third-order Butterworth high-pass filter (20 Hz) and a low-pass filter (450 Hz) to remove motion artifacts and high-frequency noise from the acquired sEMG signals, respectively. The recorded data stream was segmented into a series of analysis windows with a length of 100 ms and an overlap of 50 ms [25, 33]. Therefore, the windows were updated every 50 ms and the angle estimation frequency was 20Hz. The joint angle labels were obtained by calculating the average angle within each window [25]. To obtain training samples, each window was divided into 20 small windows

with a timestep of 5 ms, and the mean absolute value (MAV) feature of each small window was extracted. Therefore, the shape of each sample was (20, 4), where 4 represented the number of sEMG sensors.

C. Performance Evaluation

1) Evaluation Metrics

The coefficient of determination (R^2) reflects the goodness of fitting data of regression models, which was defined as

$$R^2 = 1 - \frac{\sum_{t=1}^{N}(y - y_{pre})^2}{\sum_{t=1}^{N}(y - \bar{y})^2} \tag{16}$$

where N is the number of samples, y is the ground-truth, $\bar{y}$ is the mean of y and y_{pre} is the estimated value.

Root Mean Square Error (RMSE) is a metric used to measure the deviation between estimated values and actual values, and it was defined as

$$RMSE = \sqrt{\sum_{t=1}^{N}\frac{(y - y_{pre})^2}{N}} \tag{17}$$

Due to the different range of motion in each subject's wrist, RMSE cannot accurately compare the performance of the model across subjects. We defined normalized NRMSE as

$$NRMSE = \frac{RMSE}{y_{\max} - y_{\min}} \tag{18}$$

where $y_{\max}$ and $y_{\min}$ are the maximum and minimum values of the ground-truth, respectively.

This work focused on single-to-single cross-subject estimation, each subject was considered a source or target domain, thus resulting in 90 cross-subject estimation processes. We used Si–>Sj (i, j = 1,2,…,10, i≠j) to represent the cross-subject estimation process from source subject i to target subject j. The training data for each cross-subject estimation process consisted of 60 seconds of labeled data from the source subject and 20 seconds of unlabeled data (comprising three full wrist flexion and extension exercises) from the target subject. The remaining 110 seconds of data from the target subject were used as the test set to evaluate the model. Each cross-subject estimation process was repeated five times for training to obtain the average and standard error to reduce the randomness effects.

2) Comparison Methods

Three methods were used to compare the performance of MADAN. One method was BiLSTM without any DA, which exhibited excellent performance in myoelectric continuous motion recognition without considering the domain shift [4, 5]. In addition, two representative DA methods for cross-subject myoelectric recognition were designed.

One method was the adaptive adversarial neural network (ADANN), which demonstrated outstanding performance in cross-subject gesture recognition [22]. As this work aimed to estimate joint angles, we optimized and improved the ADANN to ensure a fair comparison.

Another method was the domain-adaptive two-stream CNN with shared weights, which was currently the most advanced method for cross-subject wrist joint angle estimation [25]. We referred to it as TCDA for convenience. Although TCDA was an SDA method, the authors explained that it could also be extended to UDA by modifying the loss function.

All methods were built using PyTorch as the software framework. TABLE I presents the detailed network structure of the proposed MADAN. The grid search method was employed to determine the optimal hyperparameters, as shown in TABLE II.

TABLE I
THE NETWORK STRUCTURE OF MADAN

Name of modules	Layers
Feature extraction module	BatchNorm1d() BiGRU(hidden_size=128, num_layers=2, dropout=0.5) Linear(256)
Domain confusion module	Linear(128) ReLU() Linear(32) ReLU() Linear(2)
Joint angle estimation module	Linear(128) ReLU() Linear(32) ReLU() Linear(1)

TABLE II
THE HYPERPARAMETER OF MADAN

Hyperparameter	Value
Learning rate	Adam(1e-4)
Max_epoch	25
Batch size n_b	32
Multi-order trade-off parameter γ	1.0
Domain adversarial trade-off parameter λ	1.0

IV. RESULTS

A. Estimation Performance Comparison

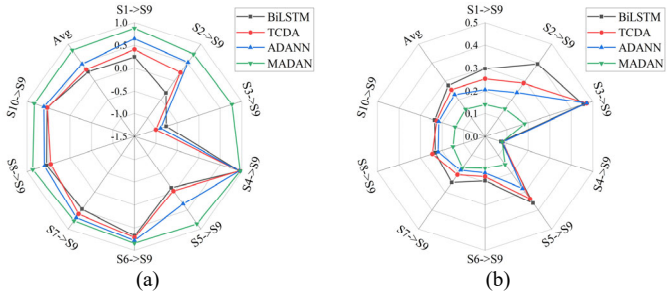

Fig. 4. Four methods to Si–>S9 (i = 1, 2,…, 8,10) of the estimated performance. (a) R^2 and (b) NRMSE.

Fig. 4 shows the R^2 and NRMSE in the cross-subject estimation with S9 as the target subject, that is Si–>S9 (i = 1, 2,…, 8,10). BiLSTM had a negative R^2 in some estimations processes, such as S2–>S9, S3–>S9 and S5–>S9, which were considered to have a significant sEMG distribution shift among these subjects. However, the performance of BiLSTM

in some estimation processes was not significantly different from the three UDA methods, such as S4–>S9 and S6–>S9, which were considered to have a slight sEMG distribution shift among these subjects. MADAN effectively improved the estimation performance for all cross-subject estimation processes, whereas TCDA and ADANN showed minor improvements, even negative improvements in S3–>S9.

To visualize the estimation performance, Fig. 5 shows the wrist angle estimation trajectories and absolute error histograms relative to the ground-truth for the four methods in S1–>S9. Fig. 5 illustrates that the estimated trajectory of BiLSTM was significantly different from the ground-truth and had a much larger absolute error than the other methods. Although the trajectories of TCDA and ADANN were closer to the ground-truth than BilSTM, the absolute errors for most of their sample points were distributed in the range of 10-60 degrees. In contrast, the trajectories of MADAN mostly coincided with the ground-truth, and the absolute errors of most sample points were distributed in the range of 10-30 degrees. In addition, the estimated trajectories of MADAN showed no degradation over time.

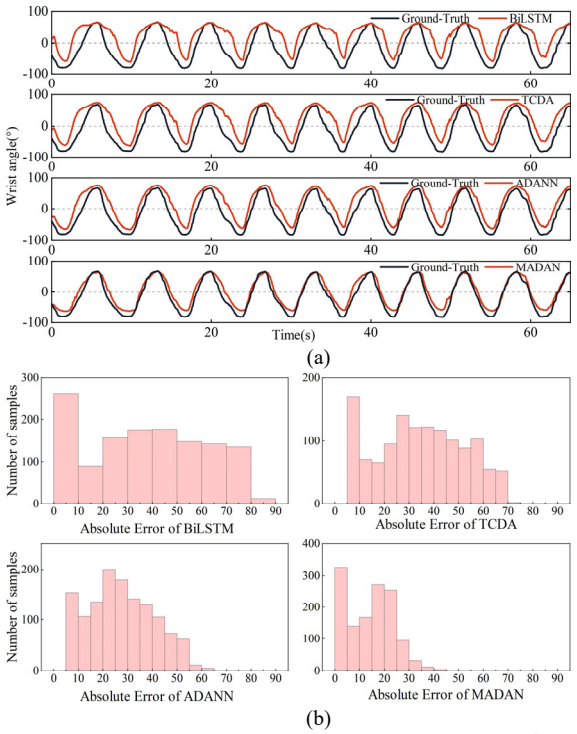

Fig. 5. (a) The wrist angle estimation trajectories of BiLSTM (R^2=0.2797), TCDA (R^2=0.4627), ADANN (R^2=0.6742) and MADAN (R^2=0.8635) in the S1–>S9. (b) The absolute error histogram for each method relative to ground-truth.

To compare the estimation performance of the four methods for all cross-subject processes, we used Tj to denote the average of the evaluation metrics for nine cross-subject estimation processes (Si–>Sj (i = 1,2...10, i≠j)) with Sj as the target subject. As shown in Fig. 6, compared with BiLSTM, TCDA and ADANN improves the cross-subject estimation performance slightly on the whole by introducing domain adaptation. However, negative improvements were observed when subjects 7 and 8 were considered as target subjects. In contrast, MADAN demonstrates significant improvements in all cross-subject estimation processes. Additionally, MADAN exhibits smaller NRMSE and RMSE values compared to other methods, with estimation errors around 15°.

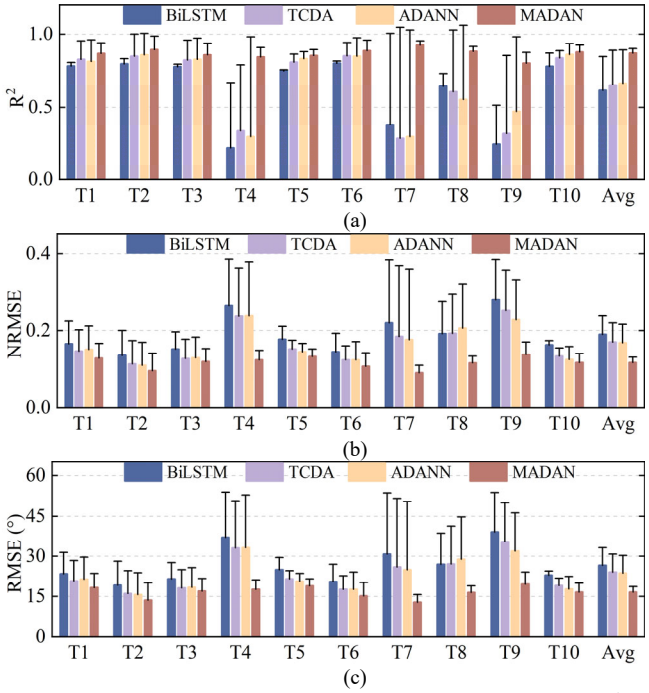

Fig. 6. Cross-subject estimation performance of the four methods. (a) R^2, (b) NRMSE and (c) RMSE.

In addition, a one-way analysis of variance (ANOVA) was applied to verify the effectiveness of MADAN further. We performed a Friedman test on the four methods' estimation performance. The p-value was less than 0.05, indicating significant differences between the four models. Subsequently, the Wilcoxon signed-rank test was applied to (MADAN, BiLSTM), (MADAN, TCDA) and (MADAN, ADANN). The results showed that MADAN (R^2=0.8688 ± 0.0307) significantly outperformed BiLSTM (R^2=0.6176 ± 0.2280, p=0.0059), TCDA (R^2=0.6534 ± 0.2341, p=0.0059) and ADANN (R^2=0.6655 ± 0.2255, p=0.0059).

B. Ablation Experiment

MADAN is a hybrid unsupervised domain adaptation method, minimizing source and target domain differences through metric-based alignment and adversarial-based confusion. To evaluate the effectiveness of these components, ablation experiments were conducted to eliminate these improvements and observe their effects. TABLE I shows the average performance of different variants on all cross-subject estimation processes. To further demonstrate the contributions of the different components, we visualized the extracted sEMG features as shown in Fig. 7. Specifically, we reduced the high-dimensional sEMG features output by the feature extractor through principal component analysis and showed their distribution using Gaussian kernel estimation. The following findings can be obtained:

(1) Metric-based domain alignment and adversarial-based domain confusion are both important components of cross-subject UDA methods, but the latter contributes more than the former.

(2) MADAN successfully eliminates the distribution discrepancy of sEMG features through the two key steps of domain adaptation and achieves distribution alignment.

TABLE III
RESULTS OF MADAN ABLATION EXPERIMENTS

Ablation variants	R^2	NRMSE
MADAN	0.8688	0.0307
− Metric-based domain alignment	0.6953	0.1536
− Adversarial-based domain confusion	0.6535	0.1684
− Hybrid domain adaptation	0.6076	0.1902

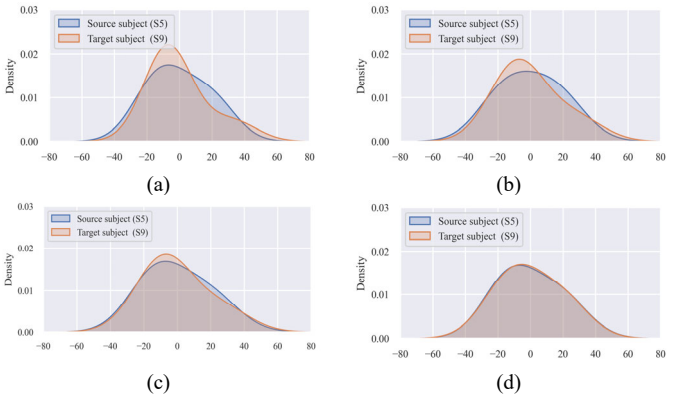

Fig. 7. Feature distribution visualization of S5–>S9. (a) MADAN without any DA, (b) MADAN without adversarial DA, (c) MADAN without metric DA, (d) MADAN.

V. DISCUSSION

A. Benefits of the proposed MADAN

Individual differences are one of the potential challenges in the practical application of sEMG interactive technology. Particularly in continuous motion estimation, new users generally need angle sensors to obtain actual joint angles as labels for model training, which undoubtedly increases training burden and cost. Therefore, this work proposes a UDA method for cross-subject myoelectric joint angle estimation, intending to help new users achieve joint angle estimation using only sEMG sensors.

BiLSTM exhibited the lowest performance, indicating that individual differences have a significant impact on the estimation performance. Compared with BiLSTM, TCDA and ADANN improved the generalization capability of the estimation model to target subjects through domain adaptation. However, the performance of TCDA and ADANN was still unsatisfactory. Moreover, Fig. 6 demonstrates that TCDA and ADANN have large standard deviations in terms of R2, NRMSE, and RMSE, indicating instability in their performance across subjects. In contrast, MADAN consistently performed well and showed stability across all subjects. Its smaller estimation errors ensured the synchronization between the subjects' joint angles and the robotic arm's joint angles, thereby enhancing the control capability over the end position.

The ablation experiments revealed that applying the metric method and adversarial method separately is insufficient to eliminate distribution differences. The proposed MADAN is a hybrid UDA method that aims to reduce the differences between the source and target subjects from two distinct domain adaptation perspectives: domain alignment and domain confusion. It first aligns the inter-domain distribution using the metric-based method and then performs domain confusion through the adversarial-based method, thereby minimizing the inter-domain distribution differences. Although the state-of-the-art method for cross-subject estimation only requires 3 seconds of data from new users for model training [25], it is a supervised method. MADAN is an unsupervised method that requires 20 seconds of sEMG data from the target subject, which allows new users to be independent of angle sensors, providing significant benefits to the users. In addition, this work used only a simple two-layer BiGRU network as the feature extraction module for MADAN. The use of advanced deep learning networks [6, 8] as feature extractors is expected to further enhance estimation performance.

B. Limitations and Future Work

Although this study has achieved excellent performance in cross-subject estimation, there are still some limitations that should be addressed in future research. For example, the experimental protocol of this study is the same as the state-of-the-art cross-subject joint angle estimation study [25], which only involves wrist flexion and extension movements. Nevertheless, the proposed method can be extended to estimate other joints in future research. When expanding to other joints, two considerations should be noted: 1) Avoid cross-joint estimation: The proposed unsupervised domain adaptation method can achieve effective cross-domain estimation only when there is correlation between the two domains. In the case of cross-subject joint estimation, this correlation refers to the similarity in muscle activation patterns among different subjects during the execution of the same limb movement. Different joints have varying ranges of motion and muscle activation patterns. Cross-joint estimation may not achieve high-performance estimation; 2)Maintain consistency in sensor data: Ensure the use of the same number of sensors attached to the corresponding muscle tissue positions, ensuring consistency in sEMG data across subjects.

Additionally, this study did not include older subjects. Although previous research has demonstrated that muscle activation patterns are not significantly affected by age [34, 35], it is advisable to conduct experiments involving older subjects in future studies to validate the effectiveness of the proposed method.

VI. CONCLUSION

This study proposes a novel hybrid UDA method for cross-subject myoelectric continuous motion estimation. The multi-

order metric and the adversarial mechanism are proposed to align domain distributions and increase domain confusion, respectively. The proposed method can achieve excellent cross-subject estimation performance with just 20 seconds of unlabeled samples from the target subject. This work enables new users to no longer rely on angle sensors or optical sensors in myoelectric continuous motion estimation. The proposed unsupervised cross-subject estimation method holds promise for improving the efficiency of myoelectric products.

REFERENCES

[1] M. D. Zheng, M. S. Crouch, and M. S. Eggleston, "Surface Electromyography as a Natural Human-Machine Interface: A Review," *IEEE Sensors Journal,* vol. 22, no. 10, pp. 9198-9214, May, 2022.

[2] P. K. Artemiadis, and K. J. Kyriakopoulos, "EMG-Based Control of a Robot Arm Using Low-Dimensional Embeddings," *IEEE Transactions on Robotics,* vol. 26, no. 2, pp. 393-398, Apr, 2010.

[3] M. Barsotti, S. Dupan, I. Vujaklija, S. Dosen, A. Frisoli, and D. Farina, "Online Finger Control Using High-Density EMG and Minimal Training Data for Robotic Applications," *IEEE Robotics and Automation Letters,* vol. 4, no. 2, pp. 217-223, Apr, 2019.

[4] L. Q. Wen, J. C. Xu, D. L. Li, X. L. Pei, and J. H. Wang, "Continuous estimation of upper limb joint angle from sEMG based on multiple decomposition feature and BiLSTM network," *Biomedical Signal Processing and Control,* vol. 80, Feb, 2023.

[5] C. F. Ma, C. Lin, O. W. Samuel, W. Y. Guo, H. Zhang, S. Greenwald, L. S. Xu, and G. L. Li, "A Bi-Directional LSTM Network for Estimating Continuous Upper Limb Movement From Surface Electromyography," *IEEE Robotics and Automation Letters,* vol. 6, no. 4, pp. 7217-7224, Oct, 2021.

[6] Y. J. Geng, Z. B. Yu, Y. C. Long, L. N. Qin, Z. Y. Chen, Y. C. Li, X. Guo, and G. L. Li, "A CNN-Attention Network for Continuous Estimation of Finger Kinematics from Surface Electromyography," *IEEE Robotics and Automation Letters,* vol. 7, no. 3, pp. 6297-6304, Jul, 2022.

[7] V. D. Silva-Acosta, I. Roman-Godinez, S. Torres-Ramos, and R. A. Salido-Ruiz, "Automatic estimation of continuous elbow flexion-extension movement based on electromyographic and electroencephalographic signals," *Biomedical Signal Processing and Control,* vol. 70, Sep, 2021.

[8] H. Lee, D. Kim, and Y. L. Park, "Explainable Deep Learning Model for EMG-Based Finger Angle Estimation Using Attention," *IEEE Transactions on Neural Systems and Rehabilitation Engineering,* vol. 30, pp. 1877-1886, Jul, 2022.

[9] A. Phinyomark, F. Quaine, S. Charbonnier, C. Serviere, F. Tarpin-Bernard, and Y. Laurillau, "A feasibility study on the use of anthropometric variables to make muscle-computer interface more practical," *Engineering Applications of Artificial Intelligence,* vol. 26, no. 7, pp. 1681-1688, Aug, 2013.

[10] B. Xue, L. Wu, K. Wang, X. Zhang, J. Cheng, X. Chen, and X. Chen, "Multiuser gesture recognition using sEMG signals via canonical correlation analysis and optimal transport," *Computers in Biology and Medicine,* vol. 130, Mar, 2021.

[11] Z. Li, X. Zhao, G. Liu, B. Zhang, D. Zhang, and J. Han, "Electrode Shifts Estimation and Adaptive Correction for Improving Robustness of sEMG-Based Recognition," *IEEE Journal of Biomedical and Health Informatics,* vol. 25, no. 4, pp. 1101-1110, Apr, 2021.

[12] P. P. K. Chan, Q. X. Li, Y. F. Fang, L. Y. Xu, K. R. Li, H. H. Liu, and D. S. Yeung, "Unsupervised Domain Adaptation for Gesture Identification Against Electrode Shift," *IEEE Transactions on Human-Machine Systems,* vol. 52, no. 6, pp. 1271-1280, Dec, 2022.

[13] T. D. Lalitharatne, K. Teramoto, Y. Hayashi, T. Nanayakkara, and K. Kiguchi, "Evaluation of Fuzzy-Neuro Modifiers for Compensation of the Effects of Muscle Fatigue on EMG-Based Control to be Used in Upper-Limb Power-Assist Exoskeletons," *Journal of Advanced Mechanical Design Systems and Manufacturing,* vol. 7, no. 4, pp. 736-751, 2013.

[14] D. Yang, W. Yang, Q. Huang, and H. Lu, "Classification of Multiple Finger Motions During Dynamic Upper Limb Movements," *IEEE Journal of Biomedical and Health Informatics,* vol. 21, no. 1, pp. 134-141, Jan, 2017.

[15] I. Batzianoulis, N. E. Krausz, A. M. Simon, L. Hargrove, and A. Billard, "Decoding the grasping intention from electromyography during reaching motions," *Journal of Neuroengineering and Rehabilitation,* vol. 15, Jun, 2018.

[16] J. Y. He, D. G. Zhang, N. Jiang, X. J. Sheng, D. Farina, and X. Y. Zhu, "User adaptation in long-term, open-loop myoelectric training: implications for EMG pattern recognition in prosthesis control," *Journal of Neural Engineering,* vol. 12, no. 4, Aug, 2015.

[17] M. B. I. Reaz, M. S. Hussain, and F. Mohd-Yasin, "Techniques of EMG signal analysis: detection, processing, classification and applications," *Biological Procedures Online,* vol. 8, pp. 11-35, Mar, 2006.

[18] D. Z. Xiong, D. H. Zhang, X. G. Zhao, and Y. W. Zhao, "Deep Learning for EMG-based Human-Machine Interaction: A Review," *IEEE-Caa Journal of Automatica Sinica,* vol. 8, no. 3, pp. 512-533, Mar, 2021.

[19] E. A. Biddiss, and T. T. Chau, "Upper limb prosthesis use and abandonment: A survey of the last 25 years," *Prosthetics and Orthotics International,* vol. 31, no. 3, pp. 236-257, Sep, 2007.

[20] S. J. Pan, and Q. A. Yang, "A Survey on Transfer Learning," *IEEE Transactions on Knowledge and Data Engineering,* vol. 22, no. 10, pp. 1345-1359, Oct, 2010.

[21] W. M. Kouw, and M. Loog, "A Review of Domain Adaptation without Target Labels," *IEEE Transactions on Pattern Analysis and Machine Intelligence,* vol. 43, no. 3, pp. 766-785, Mar, 2021.

[22] E. Campbell, A. Phinyomark, and E. Scheme, "Deep Cross-User Models Reduce the Training Burden in Myoelectric Control," *Frontiers in Neuroscience,* vol. 15, May, 2021.

[23] G. Marano, C. Brambilla, R. M. Mira, A. Scano, H. Mueller, and M. Atzori, "Questioning Domain Adaptation in Myoelectric Hand Prostheses Control: An Inter- and Intra-Subject Study," *Sensors,* vol. 21, no. 22, Nov, 2021.

[24] Y. C. Long, Y. J. Geng, C. Y. Dai, and G. L. Li, "A Transfer Learning Based Cross-Subject Generic Model for Continuous Estimation of Finger Joint Angles From a New User," IEEE Journal of Biomedical and Health Informatics, vol. 27, no. 4, pp. 1914-1925, Apr, 2023.

[25] T. Z. Bao, S. A. R. Zaidi, S. Q. Xie, P. F. Yang, and Z. Q. Zhang, "Inter-Subject Domain Adaptation for CNN-Based Wrist Kinematics Estimation Using sEMG," *IEEE Transactions on Neural Systems and Rehabilitation Engineering,* vol. 29, pp. 1068-1078, 2021.

[26] Y. J. Shi, X. H. Ying, and J. F. Yang, "Deep Unsupervised Domain Adaptation with Time Series Sensor Data: A Survey," Sensors, vol. 22, no. 15, Aug, 2022.

[27] A. Gretton, K. M. Borgwardt, M. J. Rasch, B. Scholkopf, and A. Smola, "A Kernel Two-Sample Test," *Journal of Machine Learning Research,* vol. 13, pp. 723-773, Mar, 2012.

[28] B. C. Sun, and K. Saenko, "Deep CORAL: Correlation Alignment for Deep Domain Adaptation," *Lecture Notes in Computer Science.* pp. 443-450, 2016.

[29] S. Ben-David, J. Blitzer, K. Crammer, A. Kulesza, F. Pereira, and J. W. Vaughan, "A theory of learning from different domains," *Machine Learning,* vol. 79, no. 1-2, pp. 151-175, May, 2010.

[30] Y. Ganin, and V. Lempitsky, "Unsupervised Domain Adaptation by Backpropagation," *Proceedings of Machine Learning Research.* pp. 1180-1189, 2015.

[31] Y. Ganin, E. Ustinova, H. Ajakan, P. Germain, H. Larochelle, F. Laviolette, M. Marchand, and V. Lempitsky, "Domain-Adversarial Training of Neural Networks," *Journal of Machine Learning Research,* vol. 17, 22016.

[32] C. S. Lu, C. C. Gu, K. J. Wu, S. Y. Xia, H. T. Wang, and X. P. Guan, "Deep transfer neural network using hybrid representations of domain discrepancy," *Neurocomputing,* vol. 409, pp. 60-73, Oct, 2020.

[33] T. Z. Bao, S. A. R. Zaidi, S. Q. Xie, P. F. Yang, and Z. Q. Zhang, "A CNN-LSTM Hybrid Model for Wrist Kinematics Estimation Using Surface Electromyography," *IEEE Transactions on Instrumentation and Measurement,* vol. 70, 2021.

[34] X. L. Chen, X. J. Dong, Y. E. Feng, Y. T. Jiao, J. Yu, Y. Song, X. X. Li, L. J. Zhang, P. G. Hou, and P. Xie, "Muscle activation patterns and muscle synergies reflect different modes of coordination during upper extremity movement," Frontiers in Human Neuroscience, vol. 16, Jan, 2023.

[35] V. Monaco, A. Ghionzoli, and S. Micera, "Age-Related Modifications of Muscle Synergies and Spinal Cord Activity During Locomotion," Journal of Neurophysiology, vol. 104, no. 4, pp. 2092-2102, Oct, 2010.